[10] I. S. Gradshteyn and I. W. Ryzhik, *Table of Integrals, Series, and Products*. New York: Academic Press, section 7.32, 1965.
[11] S. W. Lee, W. R. Jones, and J. J. Campbell, "Convergence of numerical solutions of iris-type discontinuity problems," *IEEE Trans. Microwave Theory Tech.*, vol. MTT-19, pp. 528–536, 1971.
[12] P. I. Somlo and J. D. Hunter, "A six-port reflectometer and its complete characterization by convenient calibration procedures," *IEEE Trans. Microwave Theory Tech.*, vol. MTT-30, pp. 186–192, 1982.
[13] P. I. Somlo, "The effect of flange loss on the reflection coefficient of reduced-height waveguide reflection standards," *IEEE Trans. Microwave Theory Tech.*, vol. MTT-27, pp. 795–797, 1979.

John D. Hunter (S'68–M'79–SM'83) received the B.E. (Hons.) and Ph.D. degrees in electrical engineering from the University of Canterbury, New Zealand, in 1967 and 1970, respectively.

He taught at the University of Canterbury from 1970–71, and then worked on electromagnetic scattering problems as a Post-Doctoral Fellow at the University of Manitoba in 1971–73. Since joining the CSIRO Division of Applied Physics in Sydney in 1973, he has been developing measurement systems at radio and microwave frequencies, with a particular interest in antenna measurements.

Theoretical Analysis of Intermodulation Distortion of Reflection-Type IMPATT Amplifiers

MOUSTAFA EL-GABALY, SENIOR MEMBER, IEEE, AND M. EZZAT EL-SHANDWILY, MEMBER, IEEE

Abstract—**The basic equations for a reflection-type IMPATT amplifier are used to derive expressions for the output when the amplifier is driven by a multifrequency input signal. The third-order intermodulation distortion is expressed and graphically presented for various diode, circuit, and signal parameters. The results provide a guideline for designing amplifiers with minimum intermodulation distortion or prescribed distortion level.**

I. INTRODUCTION

IMPATT amplifiers are used in microwave communication systems and are expected to find wide applications in millimeter-wave satellite communications. Due to the inherent nonlinearity of the device, when more than one signal is applied to the amplifier input, intermodulation components will result. Some of these components are usually within the bandwidth of the amplifier circuit and appear in the output as intermodulation distortion.

Several investigators used the Volterra series technique to analyze the small-signal nonlinearity of microwave devices [1]–[16]. The main idea in all these analyses is to represent the device by an equivalent circuit with nonlinear elements. The nonlinearity of the elements (such as conductance, capacitance, and transconductance) is represented by a power series of the applied RF voltage. Measurement of these parameters as functions of the RF voltage for the particular device used is then carried out. In IMPATT devices, the measured negative conductance and device susceptance as functions of RF voltage amplitude are usually used to determine the power-series coefficients through curve-fitting techniques. Investigations of this type suffer from two limitations. First, the process of measurement and curve fitting has to be carried out for each device to find the coefficients of the power series expansion for the device elements. Second, the effect of the physical parameters of the device (such as doping profile, dimensions, etc.) is not explicitly shown.

Recently, Best *et al.* [17] used a different approach to obtain the nonlinear response of a reflection IMPATT amplifier to the amplitude of the combined input signals in the time domain. They also used the measured nonlinear diode conductance for numerical calculations.

This paper investigates the intermodulation distortion of an IMPATT amplifier with a Read doping profile. The basic equations for the operation of the IMPATT device driven by a multifrequency RF voltage are used to obtain the output. The analysis is general, and it suffices to know the device parameters: phase delay $\omega\tau$, drift capacitance, avalanche frequency ω_a (or, equivalently, the small-signal admittance and ω_a), and the external circuit parameters to determine the intermodulation distortion. This avoids the extensive large-signal admittance measurements and the

Manuscript received June 15, 1983; revised October 31, 1983. This work was supported by the Kuwait University Research Council under Grant EE008.

M. El-Gabaly is with the Department of Electrical and Computer Engineering, University of Michigan, Ann Arbor, MI 48109, on leave from the Department of Electrical Engineering, Kuwait University, Kuwait.

M. E. El-Shandwily is with the Department of Electrical Engineering, University of Kuwait, Kuwait.

0018-9480/84/0400-0394$01.00 ©1984 IEEE

corresponding calculations of the various coefficients of the power series expansion through curve fitting that have to be carried out for individual diodes, as in [11]. As a result of the present analysis, it becomes possible to study the effect of each individual parameter on the intermodulation distortion and, consequently, a design criterion for minimum distortion can be established.

The theoretical analysis is carried out in Section II, where a Read-type IMPATT diode operating as a negative-resistance amplifier is considered. The driving RF voltage is a multifrequency signal. The analysis yields two systems of equations which are solved by successive approximations to give the output voltage as a function of frequency.

The results are graphically represented in Section III. The intermodulation distortion is displayed for various parameters of the device and circuit. These results provide a guideline for designing amplifiers with minimum distortion or prescribed distortion level.

II. Theoretical Analysis

The equivalent circuit of a one-port negative-resistance amplifier driven through a circulator is as shown in Fig. 1, where V_i is the input signal, the output signal is given by $V_d = V_r - V_i$, L_1 and C_1 are the lumped parameter representation of the microwave cavity, and G_L is the load seen by the diode.

There are four equations which describe the operation of the circuit of Fig. 1. Two equations describe the diode [18] and are called the electronic equations. These are

$$\frac{\tau_1}{2}\frac{dI_0(t)}{dt} = mI_0(t)\frac{E(t)}{E_c} \qquad \text{(for the avalanche region)} \tag{1}$$

$$E(t) = E_b - \frac{V_d(t)}{l} - \frac{1}{\epsilon\tau A}\int_{t-\tau}^{t}(\tau - t + t')I_0(t')\,dt' \qquad \text{(for the drift region)} \tag{2}$$

where

- τ_1 avalanche region transit time,
- τ drift region transit time,
- ϵ permittivity of the diode material,
- $I_0(t)$ total carrier current,
- $E(t)$ ac variation about E_c in the avalanche region,
- E_c critical field for dc breakdown,
- E_b dc field related to dc bias voltage,
- $V_d(t)$ ac voltage across the diode,
- l length of the drift region,
- A cross-sectional area of the diode,
- $m = E_c$ $[(d\alpha/dE)/\alpha]$ evaluated at E_c.

The other two equations describe the circuit in the presence of the diode, and they may be called the circuit equations. These are

$$I_d(t) = -C_d\frac{dV_d(t)}{dt} + \frac{1}{\tau}\int_{t-\tau}^{t} I_0(t')\,dt' \qquad \text{(total current)} \tag{3}$$

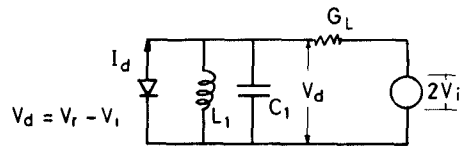

Fig. 1. Equivalent circuit of one-port negative-resistance amplifier driven through a circulator.

and

$$[2V_i(t) - V_d(t)]G_L = \frac{1}{L_1}\int V_d(t)\,dt + C_1\frac{dV_d(t)}{dt} - I_d(t) \qquad \text{(Kirchhoff's current equation)} \tag{4}$$

where

- $I_d(t)$ diode current flowing into the external circuit,
- C_d depletion-layer capacitance $= \epsilon A/l$.

The first two equations can be combined into a single equation by eliminating $E(t)$, and thus a single electronic equation is obtained

$$\frac{1}{\omega_a^2 C_d}\frac{I_0}{I_0(t)}\frac{dI_0(t)}{dt} = E_b l - V_d(t) - \frac{1}{\tau C_d}\int_{t-\tau}^{t} \cdot(\tau - t + t')I_0(t')\,dt' \tag{5}$$

where

- ω_a avalanche frequency given by $\omega_a^2 = (2mI_0/\tau_1 E_c \epsilon A)$,
- I_0 dc value of $I_0(t)$.

Similarly, the two circuit equations (3) and (4) can be combined into a single circuit equation by eliminating $I_d(t)$. The resulting equation, after differentiation with respect to time, is given by

$$2G_L\frac{dV_i(t)}{dt} = \frac{1}{L_1}V_d(t) + G_L\frac{dV_d(t)}{dt} + (C_1 + C_d)\frac{d^2V_d(t)}{dt^2} - \frac{1}{\tau}\frac{d}{dt}\int_{t-\tau}^{t} I_0(t')\,dt'. \tag{6}$$

The nonlinearity in this system of equations appears in (1) (the avalanche region) and is present in (5). Equations (5) and (6) are the required equations.

Now it is assumed that the input voltage is a multifrequency signal given by

$$V_i(t) = \sum_{n=1}^{N} S_n \cos\omega_n t \tag{7}$$

where S_n, ω_n are the amplitude and radian frequency of the nth signal. This signal can be written in the more convenient exponential form

$$V_i(t) = \frac{1}{2}\sum_{n=-N}^{N} S_n e^{j\omega_n t} \tag{8}$$

with

$$\omega_{-n} = -\omega_n, \quad S_{-n} = S_n, \quad \text{and } S_0 = 0.$$

Due to the nonlinearity of the electronic equation (5), $V_d(t)$ and $I_o(t)$ are expected to have all possible frequency

combinations. Therefore

$$V_d(t) = \frac{1}{2}\sum_l V_l e^{j\omega_l t} \tag{9}$$

$$I_0(t) = I_0 + \frac{1}{2}\sum_l I_l e^{j\omega_l t} \tag{10}$$

where

$$\omega_l = l_1\omega_1 + l_2\omega_2 + \cdots + l_N\omega_N,$$
$$V_l = V_{l_1, l_2, \cdots, l_N},$$
$$I_l = I_{l_1, l_2, \cdots, l_N},$$
$$\sum_l = \sum_{l_1=-\infty}^{\infty}\sum_{l_2=-\infty}^{\infty}\cdots\sum_{l_N=-\infty}^{\infty}, \text{ and}$$
$$V_{0,0,\cdots,0} = I_{0,0,\cdots,0} = 0.$$

Substituting (8), (9), and (10) into (5) and (6) and using the orthogonality of the exponential functions yields the following result:

$$I_l D_l = -V_l - \frac{1}{2I_0}\sum_p I_p V_{l-p} - \frac{1}{2I_0 C_d}\sum_p I_p \frac{1+j\beta p}{j\omega p} I_{l-p} \tag{11}$$

$$V_l E_l = I_l \omega_l \beta_l + 2j\omega_l G_L S_l \delta_{nl} \tag{12}$$

where

$$\delta_{nl} = 0, \quad \text{for } l \neq n$$
$$= 1, \quad \text{for } l = n$$

that is, the second term on the right-hand side of (12) is zero when it is evaluated for one of the input frequencies. The other parameters are given by

$$D_l = \frac{1}{j\omega_l C_d}\left(1 + j\beta_l - \frac{\omega_l^2}{\omega_a^2}\right)$$
$$E_l = \frac{1}{L_1} + j\omega_l G_L - (C_1 + C_d)\omega_l^2$$
$$\beta_l = \frac{1 - e^{-j\omega_l \tau}}{\omega_l \tau}.$$

The same notation is still used, i.e., l stands for $l_1, l_2, \cdots, l_N$ while n stands for one of the input components.

Successive approximations are used to obtain the output at any frequency. First, the output at the input frequencies ω_n is obtained by letting $l = 1, 0, \cdots, 0$ and $l = 0, 1, 0, \cdots, 0$ and so on, in (11) and (12). In this evaluation, the second term on the right-hand side of (11) is disregarded, while the second term on the right-hand side of (12) is counted. Thus, for the component of V_d at the frequency ω_n, the following is obtained:

$$V_{0,0,n,\cdots,0} = \frac{2j\omega_{0,0,n,\cdots,0} G_L D_{0,0,n,\cdots,0}}{(\omega\beta)_{0,0,n,\cdots,0} + (DE)_{0,0,n,\cdots,0}} S_n. \tag{13}$$

The output voltage is given by $V_{0,0,n,\cdots,0} - S_n$.

These voltages and the corresponding currents are used to obtain the second-order terms, i.e., terms with frequency $\omega_n \pm \omega_m$, where $n, m = 1, 2, \cdots, N$. The second- and first-order terms are used to obtain the third-order terms, i.e., terms with frequency $\omega_n \pm \omega_m \pm \omega_r$. Only the following two equations are written here. The output at $2\omega_1 - \omega_2$ is given by

$$V_{2,-1} = \frac{1}{(2I_0)^2 \omega_a^2 C_d} \frac{F_{1,0}^2 F_{0,-1} F_{2,-1} \beta_{2,-1} P_1 \sqrt{P_2}}{j\sqrt{2G_L} G_L^3}$$
$$\cdot \left\{ F_{1,-1}\left[\omega_{1,-1}\beta_{1,-1} + E_{1,-1}\left(-j\frac{\omega_{1,0}}{\omega_a^2 C_d} + \frac{1+j\beta_{1,-1}}{j\omega_{1,-1} C_d} \right) \right] \right.$$
$$\left. + \frac{1}{2} F_{2,0}\left[\omega_{2,0}\beta_{2,0} + E_{2,0}\left(-j\frac{\omega_{0,-1}}{\omega_a^2 C_d} + \frac{1+j\beta_{2,0}}{j\omega_{2,0} C_d} \right) \right] \right\}. \tag{14}$$

For the output at $2\omega_2 - \omega_1$, the subscripts are interchanged. The output at $\omega_1 + \omega_2 - \omega_3$ is given by

$$V_{1,1,-1}$$
$$= \frac{1}{(2I_0)^2 \omega_a^2 C_d} \frac{F_{1,0,0} F_{0,1,0} F_{0,0,-1} F_{1,1,-1} \beta_{1,1,-1} \sqrt{P_1 P_2 P_3}}{j\sqrt{2G_L} G_L^3}$$
$$\cdot \left\{ F_{0,1,-1}\left[\omega_{0,1,-1}\beta_{0,1,-1} + E_{0,1,-1}\left(\frac{-j\omega_{1,0,0}}{\omega_a 2C_d} + \frac{1+j\beta_{0,1,-1}}{j\omega_{0,1,-1} C_d} \right) \right] \right.$$
$$+ F_{1,1,0}\left[\omega_{1,1,0}\beta_{1,1,0} + E_{1,1,0}\left(\frac{-j\omega_{0,0,-1}}{\omega_a^2 C_d} + \frac{1+j\beta_{1,1,0}}{j\omega_{1,1,0} C_d} \right) \right]$$
$$\left. + F_{1,0,-1}\left[\omega_{1,0,-1}\beta_{1,0,-1} + E_{1,0,-1}\left(\frac{-j\omega_{0,1,0}}{\omega_a^2 C_d} + \frac{1+j\beta_{1,0,-1}}{j\omega_{1,0,-1} C_d} \right) \right] \right\}. \tag{15}$$

The output at $\omega_1 + \omega_3 - \omega_2$ is obtained by interchanging the second and third subscripts, and so on. F_l is given by

$$F_l = \frac{2j\omega_l G_L}{\omega_l \beta_l + E_l D_l}$$

and P_n is the input power of the signal component at frequency ω_n, given by $P_n = (S_n^2/2)G_L$.

The output powers at ω_1 and $2\omega_1 - \omega_2$ are given by

$$P_{0/p}(\omega_1) = 10\log|F_{1,0}D_{1,0} - 1|^2 + P_1 \text{ dB} \tag{16}$$

$$P_{0/p}(2\omega_1 - \omega_2) = 10\log\left(|V'_{2,-1}|^2 \frac{G_L}{2} \right) + 2P_1 + P_2 \text{ dB} \tag{17}$$

where P_1, P_2 are the input powers in decibels at ω_1 and ω_2 and $V'_{2,-1} = V_{2,-1}$.

For two-tone input with equal power and with relatively small frequency difference, the third-order intermodulation distortion IMD_3 is defined as the ratio of the third-order output power at $2\omega_1 - \omega_2$ to the output power at ω_1. From (16) and (17), it can be written as

$$IMD_3 = 10\log\left(\left|\frac{V'_{2,-1}}{F_{1,0}D_{1,0}-1}\right|^2 \frac{G_L}{2}\right) + 2P_1 \text{ dB}.$$

Numerical calculations for the amplifier gain $P_g = [P_{0/p}(\omega_1) - P_1]$ and intermodulation distortion $(IMD_3 - 2P_1)$ are carried out, and the results are presented and discussed in the next section.

III. Numerical Results and Discussion

The parameters needed to evaluate the previous expressions are 1) diode parameters $C_d, \omega_a, \omega\tau, I_0$, 2) circuit parameters L_1, C_1, G_L, and 3) input parameters ω_n, S_n.

In the following paragraphs, the effect of each set of parameters on the intermodulation distortion is studied.

A. Effect of Diode Parameters

In the following calculations, it is assumed that $\omega\tau C_d =$ const. and $(\omega_a/\omega) = KI_0^{1/2}$, where K is a constant. Keeping the same value of K and changing C_d amounts to changing the drift length, while different values of K amount to changes in the avalanche region. The circuit parameters are kept constant.

1) Effect of Drift Region: The parameters chosen for the external circuit are $L_1 = 0.8998$ nH, $C_1 = 0.643$ pF, and $G_L = 1.351$ mS. These parameters represent a practical circuit [11]. For a diode having $C_d = 0.2$ pF, $\omega\tau = 2.5$, $(\omega_a/\omega)^2 = 0.254$ at $I_0 = 30$ mA, and $f = 5.9045$ GHz, the calculated small-signal gain is 17 dB. If the diode is replaced by another with different values of C_d, while the circuit and dc bias I_0 are kept constant, then the effect on gain (P_g) and IMD_3 will be as shown in Fig. 2. The gain reaches a maximum value at $C_d = 0.18$ pF, which corresponds to $\omega\tau = 2.78$. Although the gain increases sharply as this value of C_d is reached, the intermodulation distortion IMD_3 increases at a much higher rate. For example, at $C_d = 0.2$ pF, the gain is 17 dB and $IMD_3 = 47$ dB, while at $C_d = 0.18$ pF, the gain is 29 dB and $IMD_3 = 83$ dB, i.e., for an increase in gain of 12 dB the corresponding increase in IMD_3 is 36 dB.

The effect of the dc bias I_0 is shown in Fig. 3 for a constant value of $C_d = 0.2$ pF. Both gain and IMD_3 increase with an increase in I_0. Again, the increase in IMD_3 is more pronounced than that in gain.

It is possible to keep the small-signal gain constant by changing the dc bias. This effect is shown in Fig. 4, which shows the variation of dc bias I_0 and IMD_3 with C_d for a constant gain of 15 dB. The intermodulation distortion is constant at 40 dB.

The above results indicate that, for a constant circuit, it is preferable to operate at the smallest allowable small-sig-

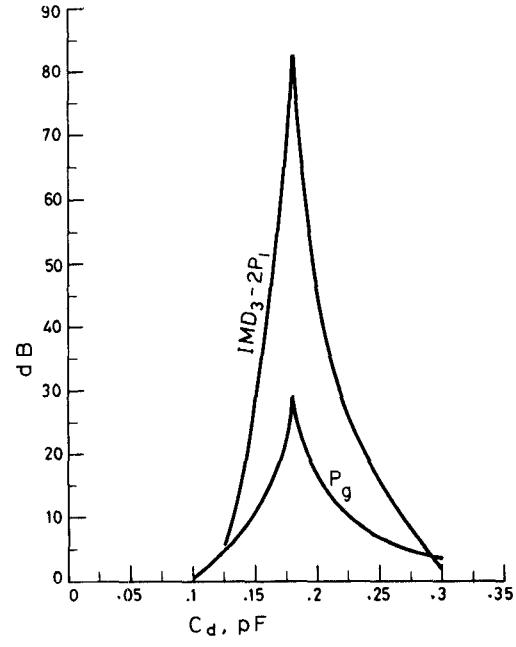

Fig. 2. Power output and IMD_3 versus C_d for constant external circuit ($I_0 = 30$ mA, $(\omega_a/\omega)^2 = 0.254$, $f_1 = 5.9045$ GHz, $f_2 = 5.9055$ GHz).

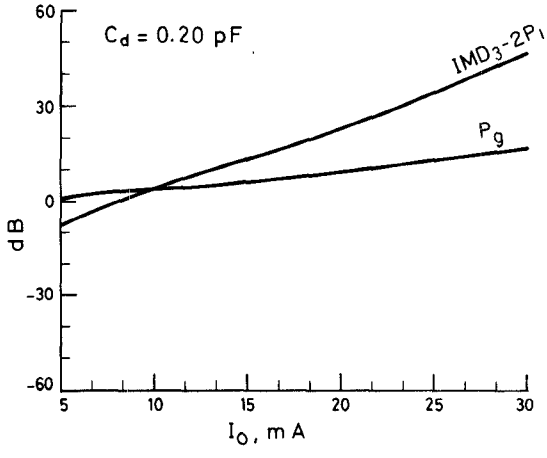

Fig. 3. Power output and IMD_3 versus I_0 for constant external circuit ($C_d = 0.2$ pF, $f_1 = 5.9045$ GHz, $f_2 = 5.9055$ GHz).

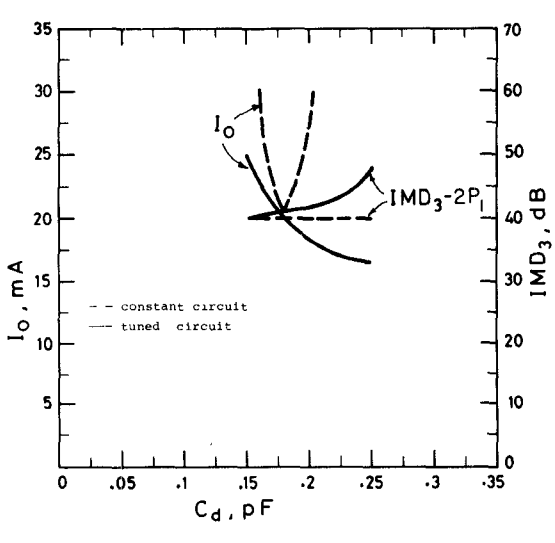

Fig. 4. I_0 and IMD_3 versus C_d for constant small-signal gain of 15 dB.

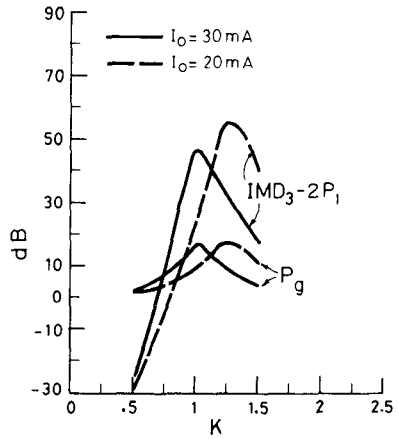

Fig. 5. I_0 and IMD_3 versus K (C_d = 0.2 pF).

nal gain to obtain the best performance as far as the intermodulation distortion is concerned.

2) Effect of Avalanche Region: This effect is shown by fixing C_d and taking different values of K. Fig. 5 shows the gain and IMD_3 as functions of K for two different values of bias I_0. It is evident that a variation in the value of K for constant C_d, I_0, and circuit parameters leads to a variation in gain and IMD_3 but without the large peaking effect, as in the case of the variation in C_d (Fig. 2). The range of K for which the gain is above 10 dB at I_0 = 30 mA is between 0.875 and 1.25, and for this range, the variation in IMD_3 is between 30 and 47 dB (Fig. 5), while the range of C_d for the same conditions is between 0.145 and 0.225 pF, and the variation in IMD_3 is between 25 and 83 dB (Fig. 2). This indicates that a replacement diode having constant C_d, to satisfy the above condition of gain, is preferable, as far as intermodulation is concerned, to one with constant K.

B. Effect of External Circuit

Fig. 6 shows the gain and IMD_3 as functions of I_0 for a diode with C_d = 0.2 pF when the equivalent load conductance G_L is kept constant and the circuit susceptance is changed to tune the diode susceptance. For these particular values of parameters, the gain and IMD_3 reach their maximum values at I_0 = 26.5 mA. Again, the reduction in IMD_3 at other values of I_0 is more pronounced than the reduction in gain.

If a diode having a different value of C_d is used and the circuit is tuned while G_L is kept constant, the gain and IMD_3 will change with C_d. To keep the gain constant, the dc bias has to be changed. Fig. 4 also shows the required variation of I_0 and the corresponding variation of IMD_3 with C_d for a gain of 15 dB. Comparing the results in Fig. 4, it is concluded that tuning the circuit increases IMD_3 by 8 dB as C_d increases from 0.15 to 0.25 pF, compared with constant IMD_3 for the constant circuit case.

C. Effect of Input Signal Parameters

The input parameters are the signal power and frequency. Since the calculations are made for an input power of 0 dB, then the remaining parameter is the signal frequency. Fig. 7 shows the intermodulation distortion versus Δf for a fixed circuit and bias and for a diode having C_d = 0.2 pF.

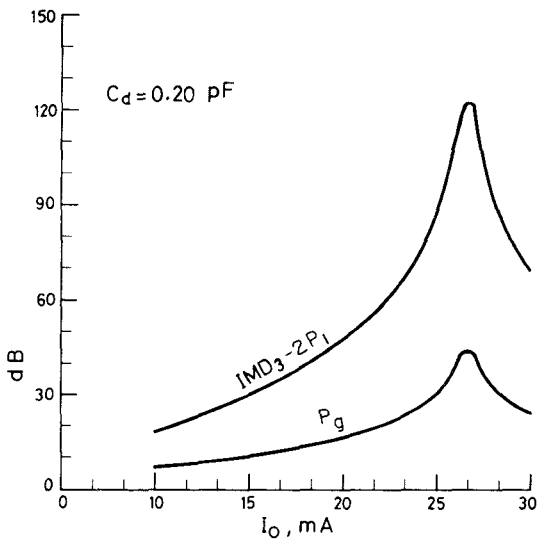

Fig. 6 Power output and IMD_3 versus I_0 for constant G_L and with circuit tuning (C_d = 0.2 pF).

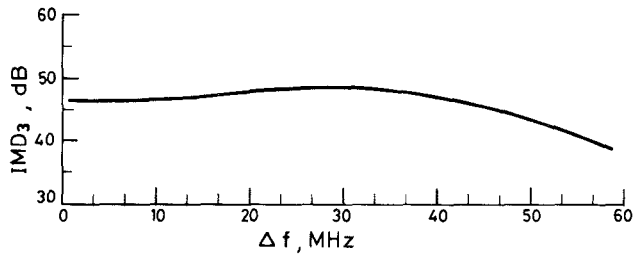

Fig. 7. IMD_3 versus frequency separation Δf (I_0 = 30 mA, C_d = 0.2 pF, gain at f_1 is constant at 17 dB).

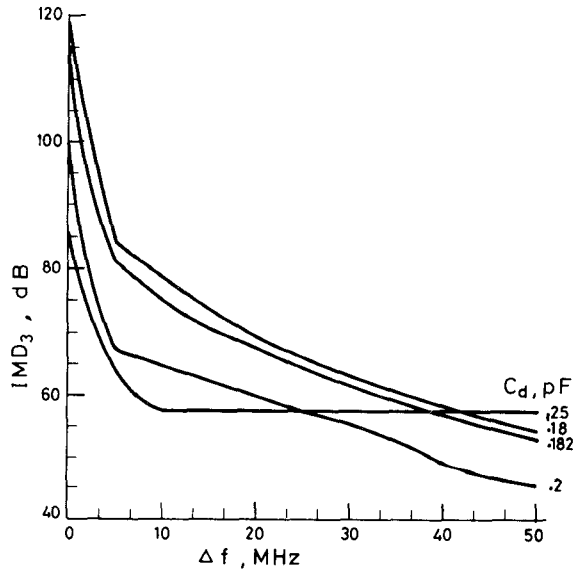

Fig. 8. IMD_3 versus frequency separation Δf (f_1 is adjusted for maximum gain, I_0 = 30 mA).

The frequencies are f_1 = 5904.5 MHz and $f_2 = f_1 + \Delta f$. The IMD_3 remains constant at 47 ± 1.5 dB up to a frequency difference of 45 MHz, after which it decreases steadily. The small-signal gain for f_1 is 17 dB. The frequency at which maximum gain occurs is 5870 MHz. The IMD_3 is due to the generated component at $2f_1 - f_2$ which is smaller than f_1 and, consequently, closer to the frequency of maximum

gain. Therefore, the expected reduction in IMD_3 with Δf is offset by the increase in gain. This is the reason for the constancy of IMD_3 with Δf. However, for large Δf (> 35 MHz), the frequency component $2f_1 - f_2$ will be smaller than the frequency of maximum gain and, therefore, IMD_3 will decrease with Δf.

Fig. 8 shows IMD_3 versus Δf when f_1 is adjusted for maximum gain. The results in this figure are much larger and decrease steadily with Δf as compared with Fig. 7. This is expected, since the gain in Fig. 8 is much larger and $2f_1 - f_2$ lies below the maximum gain frequency.

IV. Conclusions

Several conclusions can be drawn from the previous discussion.

1) For a constant circuit and bias, the replacement of the diode by one having different values of C_d will change the gain and IMD_3, but the change in IMD_3 is three times the change in gain (in decibels).

2) The dc bias can be adjusted to keep the gain and IMD_3 simultaneously constant for diodes having different values of C_d in a constant circuit.

3) The dc bias can be adjusted to keep the gain constant, but the IMD_3 will increase if the circuit is tuned above its value for the constant circuit case. Furthermore, in an amplifier circuit having constant bias, with the requirement that the gain is above a certain level, diodes having constant C_d will yield smaller intermodulation variation than diodes with constant avalanche characteristics.

4) The IMD_3 decreases monotonically with the frequency separation if one of the input frequencies is at the maximum gain. However, if f_1 and f_2 are not at the frequency of maximum gain, then IMD_3 will remain approximately constant with Δf until $f_1 - \Delta f$ equals the frequency of maximum gain.

5) It is preferable to operate the amplifier at the smallest allowable gain to obtain the best performance as far as the IMD_3 is concerned.

Acknowledgment

The authors wish to thank Prof. G. I. Haddad for his invaluable discussions.

References

[1] A. Javed, P. A. Goud, and B. A. Syrett, "Analysis of a microwave feed-forward amplifier using Volterra series representation," *IEEE Trans. Commun. Technol.*, vol. COM-25, pp. 355–360, Mar. 1977.

[2] S. Narayanan, "Transistor distortion analysis using Volterra series representation," *Bell Syst. Tech. J.*, pp. 991–1024, May–June 1967.

[3] S. Narayanan, "Intermodulation distortion of cascaded transistors," *IEEE J. Solid-State Circuits*, vol. SC-4, pp. 97–106, June 1969.

[4] R. E. Maurer and S. Narayanan, "Intermodulation distortion analysis of transistor nonlinearities with a random input," *IEEE Trans. Commun. Technol.*, vol. COM-16, pp. 701–712, Oct. 1968.

[5] A. Prochazka and R. Neuman, "High-frequency distortion analysis of a semiconductor diode for CATV applications," *IEEE Trans. Consumer Electronics*, vol. CE-21, pp. 120–129, May 1975.

[6] R. G. Meyer, M. J. Shensa, and R. Eschenbach, "Cross modulation and intermodulation in amplifiers at high frequencies," *IEEE J. Solid-State Circuits*, vol. SC-7, pp. 16–23, Feb. 1972.

[7] Y. L. Kuo, "Distortion analysis of bipolar transistor circuits," *IEEE Trans. Circuit Theory*, vol. CT-20, pp. 709–716, Nov. 1973.

[8] S. Narayanan and H. C. Poon, "An analysis of distortion in bipolar transistors using integral charge control model and Volterra series," *IEEE Trans. Circuit Theory*, vol. CT-20, pp. 341–351, July 1973.

[9] A. M. Khadr and R. H. Johnston, "Distortion in high-frequency FET amplifiers," *IEEE J. Solid-State Circuits*, vol. SC-9, pp. 180–189, Aug. 1974.

[10] R. G. Meyer and M. L. Stephens, "Distortion in variable capacitance diodes," *IEEE J. Solid-State Circuits*, vol. SC-10, pp. 47–54, Feb. 1975.

[11] A. Javed, B. A. Syrett, and P. A. Goud, "Intermodulation distortion analysis of reflection-type IMPATT amplifiers using Volterra series representation," *IEEE Trans. Microwave Theory Tech.*, vol. MTT-25, pp. 729–734, Sept. 1977.

[12] R. S. Tucker and C. Rauscher, "Modelling the third-order intermodulation-distortion properties of a GaAs FET," *Electron. Lett.*, vol. 13, pp. 508–510, Aug. 18, 1977.

[13] T. Kouno, Y. Arai, and H. Komizo, "Analysis of GaAs FET third-order intermodulation distortion," *IECE Jap.*, vol. SSD 76–69, 1977.

[14] J. A. Higgins, "Intermodulation distortion in GaAs FETs," in *IEEE Int. Microwave Symp. Dig.* (Ottawa, Canada), June 1978, pp. 138–141.

[15] R. A. Pucel, "Profile design for distortion reduction in microwave field-effect transistors," *Electron. Lett.*, vol. 14, pp. 204–206, Mar. 16, 1978.

[16] R. A. Minasian, "Intermodulation distortion analysis of MESFET amplifiers using the Volterra series representation," *IEEE Trans. Microwave Theory Tech.*, vol. MTT-28, pp. 1–8, Jan. 1980.

[17] T. C. Best, C. A. Lee, and G. C. Dalman, "Dynamic theory of intermodulation distortion," *IEEE Trans. Microwave Theory Tech.*, vol. MTT-30, pp. 729–734, May 1982.

[18] W. J. Evans and G. I. Haddad, "A large-signal analysis of IMPATT diodes," *IEEE Trans. Electron Devices*, vol. ED-15, pp. 708–717, Oct. 1968.

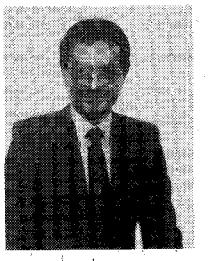

Moustafa El-Gabaly (S'70–M'74–SM'81) received the B.Sc. degree in electrical engineering and the B.Sc. degree in mathematics from the University of Cairo, Egypt, in 1965 and 1969, respectively. He received the Ph.D. degree in electrical engineering from the University of Alberta, Canada, in 1974.

During 1974 and 1975, he was with AGT, Canada, as a Design Microwave Systems Engineer. In 1976, he joined the faculty of the University of Kuwait, where he is now an Associate Professor of Electrical Engineering. He also serves as a technical consultant at Kuwait Institute of Scientific Research. During the summers of 1977 to 1980, he was a Visiting Research Scientist at the Electron Physics Laboratory, the University of Michigan, Ann Arbor. Since April 1983, he has been a Visiting Associate Professor in the Department of Electrical and Computer Engineering, the University of Michigan. His research area includes microwave solid-state devices, photovoltaic energy conversion, and photoelectronic properties of crystalline and amorphous semiconductors.

Dr. El-Gabaly received the Government of Alberta Fellowship and the National Research Council of Canada Fellowship in 1972 and 1973, respectively. He is a Professional Engineer, registered in the Province of Alberta, Canada, and is a member of the International Solar Energy Society (ISES).

M. Ezzat El-Shandwily (S'63–M'66) received the B.S.E.E. degree (honors) from Cairo University, Cairo, Egypt in 1957, and the M.S., E.E., M.Sc. (physics), and Ph.D. degrees in electrical engineering, all from the University of Michigan, Ann Arbor, in 1961, 1964, and 1965, respectively.

From 1965–1974, he was a Research Engineer in the Electrical and Electronics Engineering Laboratory, National Research Center, Cairo, Egypt, engaged in research in the field of microwave theory and techniques. From 1974 to 1980, he was with the Electrical Engineering Department, University of Technology, Baghdad, Iraq, as an Associate Professor and Professor. In 1980, he joined the Electrical Engineering Department, Kuwait University, Kuwait, as a Professor. His current research interest involves microwave solid-state devices and analysis of electromagnetic fields in anistropic media.